# Paraxial mesoderm specifies zebrafish primary motoneuron subtype identity

**Katharine E. Lewis* and Judith S. Eisen†**

Institute of Neuroscience, 1254 University of Oregon, Eugene, OR 97403, USA
*Present address: Department of Anatomy, Cambridge University, Downing Street, Cambridge CB2 3DY, UK
†Author for correspondence (e-mail: eisen@uoneuro.uoregon.edu)

*Accepted 12 November 2003*

Development 131, 891-902
Published by The Company of Biologists 2004
doi:10.1242/dev.00981

## Summary

**We provide the first analysis of how a segmentally reiterated pattern of neurons is specified along the anteroposterior axis of the vertebrate spinal cord by investigating how zebrafish primary motoneurons are patterned. Two identified primary motoneuron subtypes, MiP and CaP, occupy distinct locations within the ventral neural tube relative to overlying somites, express different genes and innervate different muscle territories. In all vertebrates examined so far, paraxial mesoderm-derived signals specify distinct motoneuron subpopulations in specific anteroposterior regions of the spinal cord. We show that signals from paraxial mesoderm also control the much finer-grained segmental patterning of zebrafish primary motoneurons. We examined primary motoneuron specification in several zebrafish mutants that have distinct effects on paraxial mesoderm development. Our findings suggest that in the absence of signals from paraxial mesoderm, primary motoneurons have a hybrid identity with respect to gene expression, and that under these conditions the CaP axon trajectory may be dominant.**

Key words: Somites, Motoneurons, MiP, CaP, Zebrafish, Spinal cord, Trilobite, Knypek, No tail, Spadetail, Fused somites, You-too, After eight, b380, b567

## Introduction

The vertebrate nervous system consists of many specialized cell types that form at distinct characteristic positions. We investigated how neurons acquire appropriate, position-specific fates by studying how primary motoneurons (PMNs), the first motoneurons (MNs) to form in the zebrafish spinal cord, are specified and patterned.

In zebrafish, as in other vertebrates, Hedgehog signals from the embryonic midline induce MNs in the ventral neural tube on both sides of the floor plate (Eisen, 1999; Lewis and Eisen, 2001). In all vertebrates examined so far, additional signals from paraxial mesoderm then specify distinct subpopulations of MNs that occupy specific motor columns at particular anteroposterior (AP) axial levels (Eisen, 1999; Ensini et al., 1998; Liu et al., 2001). For example, lateral motor column MNs are generated only at limb levels and visceral MNs are generated at thoracic levels.

Embryonic zebrafish have individually identifiable MNs, facilitating analysis of mechanisms that pattern neurons at the level of single cells. In addition to distinct motor columns at particular AP axial levels (Eisen, 1994), zebrafish also have a more fine-grained, segmentally reiterated pattern of different PMN subtypes along the spinal cord AP axis. Such a fine-grained, reiterated pattern of distinct MN subtypes has not yet been described in other vertebrates, probably because there are many more MNs, and individual cells cannot be recognized. Zebrafish have three different PMN subtypes: rostral primary (RoP), middle primary (MiP) and caudal primary (CaP). One PMN of each subtype forms per spinal hemisegment, with the exception that about half the hemisegments initially have two CaP-like PMNs, one of which is called variably present (VaP) and usually dies (Lewis and Eisen, 2003). Each PMN subtype is uniquely identifiable by soma position relative to overlying somites and by axon trajectory. For example, MiP and RoP somata are adjacent to overlying somite boundaries and CaP somata are adjacent to overlying somite middles (e.g. Fig. 1E,J). CaP axons project into ventral myotome, MiP axons project into dorsal myotome and RoP axons project into medial myotome (e.g. Fig. 1T,Z). Although many aspects of PMN development have been characterized (Lewis and Eisen, 2003), it is still unclear how these different subtypes are specified.

PMNs can first be identified molecularly by expression of *islet1*. Prospective PMNs express *islet1* soon after birth; at mid-somitogenesis stages CaPs initiate expression of *islet2* and then within 1 hour downregulate expression of *islet1*. By contrast, MiPs and RoPs never express *islet2* (Appel et al., 1995; Inoue et al., 1994; Tokumoto et al., 1995), but can be distinguished by their temporal expression of *islet1*: RoPs express *islet1* later than MiPs or CaPs (Appel et al., 1995). Therefore, at mid-somitogenesis stages CaPs can be identified by *islet2* expression and MiPs by *islet1* expression (see Fig. 1); RoPs do not yet express *islet1*.

The tight spatial correlation between the reiterated pattern of PMNs and the overlying somites suggests that signals from paraxial mesoderm might specify different PMN subtypes. Consistent with this idea, transplantation experiments have shown that environmental signals can specify zebrafish PMN subtypes (Appel et al., 1995; Eisen, 1991). For example, when

MiP is transplanted 2-3 hours before axogenesis to the position where CaP normally develops, the transplanted cell forms a CaP-like axon and initiates expression of *islet2*. However, when MiP is transplanted in the same way just 1 hour before axogenesis, it remains committed to its original fate, extends a MiP-like axon and does not express *islet2* (Appel et al., 1995; Eisen, 1991). Furthermore, PMN specification and development is disturbed in *spadetail* (*spt*) mutants, which have a dramatic reduction of trunk paraxial mesoderm (Bisgrove et al., 1997; Eisen and Pike, 1991; Inoue et al., 1994; Tokumoto et al., 1995); when somite segmentation is disturbed by heat shock, the position and axonal morphology of PMNs are also disturbed (Kimmel et al., 1988; Roy et al., 1999).

Together these observations suggest that signals from paraxial mesoderm may specify PMN subtypes. To test this hypothesis, we investigated PMN subtype specification in several zebrafish mutants that affect paraxial mesoderm development in different ways. We concentrated on MiP and CaP specification because these PMNs can be identified both molecularly and by axon trajectory. Our findings demonstrate that signals from paraxial mesoderm are required to specify MiPs and CaPs, and they suggest that additional signals from the somites are also required to fine-tune or maintain correct spatial organization of PMN subtypes.

## Materials and methods

### Propagation and identification of wild-type and mutant zebrafish embryos

Zebrafish (*Danio rerio*) embryos were obtained from natural spawnings of wild types (AB) or crosses of identified carriers heterozygous for specific mutations. Fish were maintained in the University of Oregon Zebrafish Facility on a 14 hour light/10 hour dark cycle at 28.5°C and embryos staged according to Kimmel (Kimmel, 1995) by number of somites or hours post fertilization at 28.5°C (hpf). Production of parental fish heterozygous for mutations at two different loci was carried out as in Lewis and Eisen (Lewis and Eisen, 2001). Mutant embryos were identified by morphology, except for *fss;yot* mutants younger than 24 hpf. At these stages the *fss* phenotype masks the *yot* phenotype. However, *yot* mutants lack lateral floor plate (Odenthal et al., 2000), so young *fss;yot* mutants were identified by *fss* morphology and lack of expression of a lateral floor plate marker *nkx2.2b* (kindly provided by M. Schäfer and C. Winkler prior to publication).

### Mutant alleles used in this study

*Df*(*LG12*)*dlx3b*$^{b380}$ (hereafter referred to as *Df*$^{b380}$) is a deficiency on linkage group 12 that removes 21-24 cM that includes *dlx3b*, *dlx4b*, *sox9a*, *irbp*, *rbp4* and *dkk1* (Fritz et al., 1996; Liu et al., 2003). *Df*(*LG05*)*her1*$^{b567}$ (hereafter referred to as *Df*$^{b567}$) is a deficiency on linkage group 5 that removes up to 22 cM that includes *her1*, *her7*, *ndr3* and a number of ESTs (Henry et al., 2002). Other lines used were: *after eight*$^{tr233}$ (*aei*); *fused-somites*$^{te314}$ (*fss*); *you-too*$^{ty17}$ (*yot*) (van Eeden et al., 1996); *no tail*$^{b195}$ (*ntl*) (Halpern et al., 1993); *spadetail*$^{b104}$ (*spt*) (Ho and Kane, 1990); *trilobite*$^{m209}$ (*tri*) (Hammerschmidt et al., 1996); *knypek*$^{b639}$ (*kny*) (Topczewski et al., 2001); *cyclops*$^{b16}$ (*cyc*) (Hatta et al., 1991); and *floating head*$^{n1}$ (*flh*) (Talbot et al., 1995).

### PMN subtype assays

All analyses were carried out on PMNs in the trunk except that PMNs in the tail were analysed where noted in the text. Whenever possible, we assayed CaP and MiP identity using both axon trajectory (znp1 antibody staining) at 26-30 hpf and gene expression (*islet1* and *islet2*) at 17-19 hpf, when MiPs, which are located directly under somite boundaries express *islet1* (Fig. 1E) and CaPs, which are located under somite middles express *islet2* (Fig. 1J). In all cases we examined at least seven embryos in detail using a compound microscope, and in several cases we analysed both whole mounts and serial cross-sections. *islet1* + *islet2* double in situ RNA hybridization did not provide strong enough signals to assess gene expression unequivocally. Therefore, to determine the distribution of *islet1*-expressing and *islet2*-expressing PMNs, we conducted in situ RNA hybridization for each gene alone as well as Islet antibody staining followed by *islet2* in situ RNA hybridization (Fig. 1). The Islet antibody recognizes both Islet1 and Islet2. Therefore, PMNs recognized by both Islet antibody and *islet2* riboprobe express *islet2* and hence are CaPs, whereas PMNs recognized by Islet antibody alone only express Islet1 and are MiPs (Fig. 1O). In some mutants most or all PMNs expressed *islet2*; comparison with *islet1* in situ RNA hybridization suggested that many of them also expressed *islet1*. Therefore, these PMNs had a hybrid identity. In these cases we examined how many PMNs expressed *islet1* by Islet antibody staining followed by *islet1* in situ RNA hybridization; PMNs labeled by antibody alone express only Islet2, whereas PMNs labeled by antibody and *islet1* riboprobe express *islet1* (Fig. 1Y). We were able to identify cells that expressed only *islet1*, only *islet2*, or both *islet1* and *islet2* unequivocally using this combination of markers.

### In situ RNA hybridization and antibody staining

In situ RNA hybridization was performed as previously described (Concordet et al., 1996). *her1* probe was synthesized as described by Müller (Müller, 1996), *cs131* probe was synthesized as described by Durbin et al. (Durbin et al., 2000), and *islet1* and *islet2* probes were synthesized as described by Appel et al. (Appel et al., 1995). Islet antibodies originally isolated by the Jessell Laboratory were obtained from the Developmental Studies Hybridoma Bank developed under the auspices of the NICHD and maintained by the University of Iowa, Department of Biological Sciences, Iowa City, IA 52242. Antibody 39.4D5 was used alone at a final concentration of 1/200 or a 1:1 mixture of 39.4D5 and 40.2D6 was used; in the latter case, both antibodies were used at a final concentration of 1/300. In cases in which Islet antibody staining and *islet1* or *islet2* in situ RNA hybridization were performed on the same embryos, antibody staining was carried out first. Embryos were fixed for 5-6 hours at 4°C in 4% PFA in PBS, permeabilized by washing with PBS + 0.5% Triton for several hours and distilled $H_2O$ for 30 minutes and blocked in a serum-free block solution [2% BSA; 1×PBS; 5-10% DMSO; 0.2% Triton plus RNAse inhibitor (20-40 units/ml)] for 1 hour. Embryos were then incubated with Islet antibody in fresh serum-free block overnight at 4°C. Antibody staining was developed using the Sternberger Clonal PAP system and detected using a Vector Laboratories DAB kit. The same serum-free block was used for secondary and tertiary antibodies. Embryos were then fixed for 15-20 minutes in 4% PFA in PBS and processed for in situ RNA hybridization.

Axon trajectories were assessed as described by Eisen et al. (Eisen et al., 1989) using znp1 monoclonal antibody (Trevarrow et al., 1990), the Sternberger Clonal PAP system and Vector Laboratories DAB kit. In all cases, CaP axons were clearly visible both in whole mount and in cross-section. In some mutants, MiP axons were easier to identify in cross-section.

Specimens were analysed using a Zeiss Axioplan microscope and photographed with Kodak Ektachrome 64T or 164T film. Images were scanned on a Nikon LS-1000 35mm film scanner and processed using Adobe Photoshop software.

### Morpholino injections

Morpholino antisense oligonucleotides (MOs) were obtained from Gene Tools. About 5 nl of a MO mix (*ntl* MO 1 mg/ml; *spt* MO #1 0.75 mg/ml; *spt* MO #2 0.075 mg/ml) was injected into one- to two-

cell wild-type embryos. This concentration reliably phenocopied *ntl;spt* mutants. The MO sequences were: *ntl* MO, GACTTG-AGGCAGGCATATTTCCGAT (see also Nasevicius and Ekker, 2000); *spt* MO #1, AGCCTGCATTATTTAGCCTTCTCTA; and *spt* MO #2, GATGTCCTCTAAAAGAAAATGTCAG.

### Transplantation

For all blastula stage transplants and some somite transplants we used *ntl;spt* MO-injected embryos as hosts. We confirmed that MO-injected embryos phenocopy *ntl;spt* mutants by examining their morphology, *islet1* and *islet2* expression patterns and *tropomyosin* expression (to confirm absence of somitic mesoderm).

### Blastula stage transplants

Wild-type donor embryos were injected with a mixture of 2.5% 3 kDa fluorescein dextran and 2.5% 3 kDa rhodamine dextran in 0.2M KCl at the one- to two-cell stage. Host embryos were injected with a mixture of *ntl* and *spt* MOs at the one- to two-cell stage. Fluorescently labeled, wild-type cells were transplanted into the margin of *ntl;spt* MO-injected embryos between blastula and 30% epiboly stages (Fig. 6A); embryos were analysed and fixed at 18-22 somites.

### Whole somite transplants

We transplanted fluorescently labeled whole somites from wild-type donors at the 7- to 10-somite stage into similarly staged *ntl;spt* mutant or *ntl;spt* MO-injected hosts (Fig. 6E); results were identical in both cases. These experiments need to be done early enough that PMN subtype identities are still labile (Appel et al., 1995; Eisen, 1991); this was possible because *ntl;spt* mutants completely lack somitic mesoderm (Amacher et al., 2002) and therefore we did not need to remove somites from host embryos. Fluorescently labeled wild-type donor somites were prepared as described previously (Beattie and Eisen, 1997). Donors were dissociated and somites, recognized by their characteristic morphology, were removed to a separate culture dish. *ntl;spt* mutants or *ntl;spt* MO-injected hosts were mounted in agar with their spinal cords facing up. Several wild-type somites were inserted into the trunk using a wide-bore micropipette (Fig. 6E). Host embryos were cultured at 28.5°C for about 4 hours in L15 medium with 50 units/ml of penicillin and 0.05 mg/ml streptomycin before being fixed for analysis. PMN identity was assayed using Islet antibody and *islet2* riboprobe. In some cases, we were able to see PMN labeling through the transplanted somites (see Fig. 6E). However, in many cases we had to remove the somites to assay PMN identity because the Fast Red stain we used to recognize donor somites obscured PMN labeling.

### Intracellular labels

Individual PMNs were labeled in live embryos (Eisen et al., 1989).

## Results

### *trilobite;knypek* double mutants have narrow somites and hybrid PMNs

If PMN subtypes are specified by signals from paraxial mesoderm, altering the relationship between somites and PMNs should change PMN subtype identities. *trilobite;knypek* (*tri;kny*) mutants have defects in convergence and extension

**Table 1. Mutants and their phenotypes**

| Mutant | Locus | Somite phenotype | References |
|---|---|---|---|
| *after-eight* (*aei*) | *deltaD* | The first eight or so somites form normally, more posterior somites do not form proper somite boundaries, although the myotome still shows later morphological segmentation | (van Eeden et al., 1996)<br>(Holley et al., 2000) |
| *cyclops* (*cyc*) | *nodal-related 2* (*ndr2*) | None | (Sampath et al., 1998)<br>(Rebagliati et al., 1998) |
| *Df*(*LG12*)*dlx3b*$^{b380}$<br>deficiency including *dlx3b*, *dlx4b*, *sox9a*, *irbp*, *rbp4* and *dkk1* | | No somite boundaries, although the myotome still shows later morphological segmentation | (Liu et al., 2003)<br>(Fritz et al., 1996) |
| *Df*(*LG05*)*her1*$^{b567}$<br>deficiency including *her1*, *her7* and *ndr3* | | Irregular somite widths and somite boundaries, as well as later morphological segmentation of myotome | (Henry et al., 2002) |
| *floating head* (*flh*) | *floating head*<br>(previously called Znot) | Misshapen somites | (Talbot et al., 1995) |
| *fused somites* (*fss*) | *tbx22* | No somite boundaries initially, but later morphological segmentation of myotome | (van Eeden et al., 1996)<br>(Nikaido et al., 2002) |
| *fss;yot* | | No somite boundaries or later morphological segmentation of myotome | (van Eeden et al., 1998) |
| *knypek* (*kny*) | *knypek*<br>(a glypican) | Narrow somites | (Topczewski et al., 2001) |
| *notail* (*ntl*) | *ntl*<br>(*brachyury*) | Somites are blocky and lack chevron shape | (Halpern et al., 1993)<br>(Schulte-Merker et al., 1994) |
| *ntl;spt* | | No paraxial mesoderm or somites | (Amacher et al., 2002) |
| *spadetail* (*spt*) | *tbx16* | Reduced trunk somites | (Ho and Kane, 1990)<br>(Griffin et al., 1998) |
| *trilobite* (*tri*) | *vangl2*<br>(also called *van gogh* and *strabismus*) | Narrow somites | (Hammerschmidt et al., 1996)<br>(Sepich et al., 2000)<br>(Jessen et al., 2002) |
| *tri;kny* | | Very narrow somites (only ~two cells wide) | (Henry et al., 2000) |
| *you-too* (*yot*) | Dominant negative allele of *gli2* | No slow muscle | (van Eeden et al., 1996)<br>(Lewis et al., 1999)<br>(Karlstrom et al., 2003) |

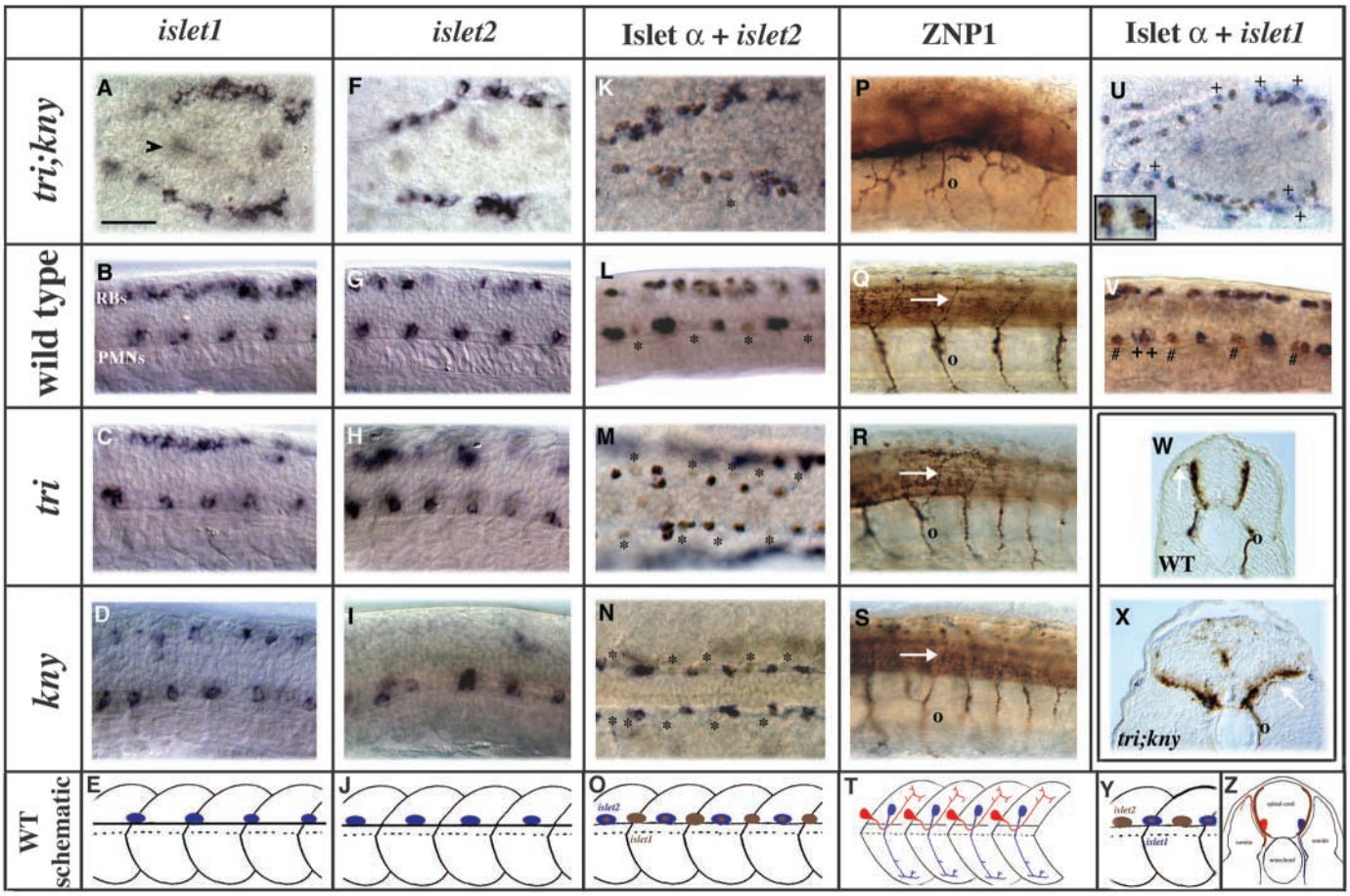


**Fig. 1.** PMNs in *tri;kny* double mutants have hybrid identities. (A-D) *islet1* RNA in situ hybridization at17-18 hpf. Dorsal view of *tri;kny* mutant (A) and lateral views of wild-type embryo (B), *tri* (C) and *kny* (D) mutants. The morphology of *tri;kny* mutants makes it difficult to obtain lateral views at these early stages. In lateral views, PMNs are ventral; dorsal cells are Rohon Beard sensory neurons (RBs) (see B). In dorsal views, all cells are PMNs; RBs are more lateral and outside the edges of these images. In wild types and single mutants, *islet1*-expressing PMNs (MiPs) are regularly spaced and their cell bodies are directly adjacent to the overlying somite boundaries (see schematic in E). In *tri;kny* mutants, *islet1*-expressing PMNs form almost continuous rows. In addition to the two major rows of PMNs, we also sometimes see some *islet1*-expressing and *islet2*-expressing cells more medial and slightly dorsal (arrowhead in A). Cross-sections (not shown) suggest that these PMNs form above a broader than normal floorplate. (E) Schematic of *islet1* in situ hybridization showing MiPs adjacent to overlying somite boundaries. (F-I) *islet2* in situ hybridization at 18-20 hpf. Dorsal view of *tri;kny* mutant (F) and lateral views of wild-type embryo (G), *tri* (H) and *kny* (I) mutants. In wild types and single mutants, *islet2*-expressing PMNs (CaPs) are adjacent to the middle of overlying somites (see schematic in J). In *tri;kny* mutants, *islet2*-expressing PMNs form almost continuous rows. (J) Schematic of *islet2* in situ hybridization showing CaPs adjacent to overlying somite middles. (K-N) Islet antibody + *islet2* in situ hybridization at 18-21 hpf. Dorsal view of *tri;kny* mutant (K) and lateral views of wild-type embryo (L) *tri* (M) and *kny* (N) mutants. Islet antibody staining is nuclear and brown; *islet2* RNA is blue and cytoplasmic (see schematic in O). Brown-only cells (*) express only *islet1* and hence are MiPs; blue + brown cells express *islet2* and possibly also *islet1*; these cells are either CaPs or hybrid PMNs. Comparison of double staining and single in situ hybridization shows that MiPs and CaPs are specified relatively normally in both single mutants. By contrast, the vast majority of PMNs in *tri;kny* mutants express *islet2* (only one brown-only cell in K). (A) Shows that at least most of these PMNs also express *islet1*; this is confirmed by Islet antibody + *islet1* in situ hybridization staining (U). (O) Schematic of Islet antibody + *islet2* in situ hybridization. (P-S) znp1 antibody staining at 26-30 hpf. Lateral views of whole-mount wild-type embryo (Q), *tri;kny* (P), *tri* (R) and *kny* (S) mutants. Ventral CaP axons are clearly visible in all cases (examples indicated with circle). In wild-type embryos, and *tri* and *kny* mutants, MiP axons are visible in whole mounts (examples indicated with white arrow). However, MiP axons are very rare in *tri;kny* mutants and can be identified only in cross-section (X). (T) Schematic of a lateral view showing ventral CaP (blue) and dorsal MiP (red) axon trajectories. (U,V) Islet antibody + *islet1* in situ hybridization at 18-21 hpf. Dorsal view of *tri;kny* mutant (U) and lateral view of wild-type embryo (V). In these embryos, brown-only cells express only *islet2* and are therefore CaPs (#). Blue + brown cells express *islet1*, but possibly also *islet2*, and are therefore MiPs, or CaPs that have not yet completely downregulated *islet1*, or hybrid PMNs. We also see occasional cells that are blue only (+). These are probably RoPs or SMNs that have started to express *islet1* RNA but not Islet protein. In *tri;kny* mutants (U), all of the PMNs express *islet1* and have blue staining. The insert shows a higher magnification view of two of these PMNs. *There are no brown-only cells* (W,X) znp1 antibody staining at 26-30 hpf. Cross-sections of wild-type embryo (W) and *tri;kny* mutant (X). Ventral CaP axons (black circle) and dorsal MiP axons (white arrow) are visible in both cases. The MiP axon hugs the lateral surface of the spinal cord as shown in the schematic (Z). (Y) Schematic of Islet antibody + *islet1* in situ hybridization staining. (Z) Schematic of a cross-section showing CaP (blue) and MiP (red) axon trajectories. The brown shading indicates znp1 immunoreactivity at the lateral surface of the spinal cord, caused by other znp1-immunoreactive spinal cord axons. Scale bar: 50 μm.

**Table 2. PMN phenotypes in mutants with narrow or absent somites**

| Genotype | Number of embryos counted | Total number of blue+brown cells | Total number of brown only cells | % of PMNs expressing only *islet1* |
|---|---|---|---|---|
| Wild type | 6 | 206 | 128 | 38% |
| *tri;kny* | 14 | 509 | 33 | 6% |
| *tri* | 7 | 209 | 127 | 38% |
| *kny* | 9 | 242 | 155 | 39% |
| *spt* | 7 | 265 | 55 | 17% |
| *ntl;spt* | 5 | 567 | 24 | 4% |

For each of the genotypes shown above, we counted PMNs in embryos stained with Islet antibody (brown nuclear staining) and *islet2* riboprobe (blue cytoplasmic staining). In these experiments, brown-only cells expressed only *islet1* (and hence were MiPs); brown+blue cells expressed *islet2* and possibly also *islet1* (and hence were CaPs or hybrid PMNs).

that result in very narrow somites that have normal AP patterning but are only about two cells wide along the AP axis (Table 1); wild-type somites are about five cells wide (Henry et al., 2000). If PMNs form in these mutants, all of them will be next to both a somite boundary and a somite middle. Therefore, we reasoned that if our hypothesis that localized signals from overlying somites specify PMN subtypes is correct, all PMNs in these mutants should be exposed to the same signals and therefore have the same subtype identity.

MiPs and CaPs form normally in *tri* and *kny* single mutants that have somites that are three or four cells wide, which is intermediate between wild types and *tri;kny* double mutants. However, PMNs are often slightly closer together in these single mutants, corresponding to the slightly narrower somites (Fig. 1C,D,H,I,M,N,R,S; Table 2). By contrast, *tri;kny* mutants have continuous stretches and clumps of PMNs, possibly because of their more severe defects in convergence and extension (Fig. 1A,F,K,U). Most PMNs in double mutants express both *islet1* and *islet2* and hence have a hybrid identity, at least in terms of gene expression (Fig. 1A,F,K,U; Table 2). None of the PMNs in *tri;kny* mutants expresses only *islet2* ($n$=8; Fig. 1U), but in some double mutants there are a few PMNs that apparently express *islet1* alone (<10% of the PMNs in any one embryo; 4/16 embryos had no *islet1* only cells). However, these could be later-forming secondary motoneurons (SMNs) that are just initiating *islet1* expression (Appel et al., 1995).

*tri;kny* mutants have many ventrally projecting CaP-like axons, although these axons have some aberrant branches. By contrast, dorsally projecting MiP-like axons are very rare and can be best seen in cross-section (Fig. 1P,X). In seven double mutants analysed in cross-section, we saw 122 CaP axons, four fairly normal MiP axons (e.g. Fig. 1X) and four shorter dorsal axons that were less convincingly MiPs. This suggests that nearly all PMN axons in *tri;kny* mutants are CaP like. We confirmed this result by dye-labeling PMNs in 14 live embryos. In contrast to wild-type embryos in which PMNs are readily identified by soma position (Eisen et al., 1989), the unusual morphology of *tri;kny* double mutant embryos makes it difficult to identify PMNs unambiguously using these criteria. Therefore, we labeled essentially every cell of the right size in the ventral spinal cord. We saw 36 CaPs, 10 PMNs with short CaP-like axons and two MiPs (both in the same embryo).

Because CaPs normally have turned off *islet1* expression by the time they extend axons, our results suggest that in *tri;kny* mutants most PMNs have a hybrid identity with respect to gene expression but a CaP-like identity based on axon trajectory. This is consistent with our hypothesis that signals from somites specify MiPs and CaPs. The simplest interpretation of our results is that in wild types there are two spatially separated signals: one that specifies MiPs and one that specifies CaPs, whereas in *tri;kny* mutants the narrow somites cause these signals to overlap so all PMNs are exposed to both signals. However, it is also possible that these mutations affect somites and PMNs independently. Therefore, to test further the hypothesis that signals from somites specify MiPs and CaPs, we examined PMN subtype specification in mutants that lack proper somite segmentation.

## MiPs and CaPs form in somite segmentation mutants

Several zebrafish mutations disturb somite segmentation and block formation of at least some somite boundaries (Fritz et al., 1996; Henry et al., 2002; Liu et al., 2003; van Eeden et al., 1996b). In all of these mutants examined so far, genes that are normally AP restricted within individual somites are either missing or ubiquitously expressed within the somitic mesoderm (Durbin et al., 2000; Henry et al., 2002; Holley et al., 2000; Jiang et al., 2000; van Eeden et al., 1996). We reasoned that if localized signals emanating from somites specify PMN subtypes, these signals might be missing or mislocalized in these mutants. Therefore, we examined MiP and CaP specification in several mutants that affect somite segmentation.

*fused somites* (*fss*) and $Df^{b380}$ mutants lack all somite boundaries (Liu et al., 2003; van Eeden et al., 1996) (Table 1). *after eight* (*aei*) mutants resemble *fss* mutants in the posterior trunk, but the first eight or so somites form normally and *aei* is thought to be involved in a different step in somite formation than *fss* (Durbin et al., 2000; Holley et al., 2000; Jiang et al., 2000) (Table1). $Df^{b567}$ mutants form somites with irregular widths and boundary defects (Henry et al., 2002) (Table 1). Despite their defects in somite boundary formation, *fss*, $Df^{b380}$, *aei* and $Df^{b567}$ mutants all form myotome boundaries at later stages, although these are irregular (Henry et al., 2002; van Eeden et al., 1998) (K.E.L. and J.S.E., unpublished). We therefore also analysed *fused somites;you-too* (*fss;yot*) mutants because they lack even this later morphological segmentation of somitic mesoderm (van Eeden et al., 1998) (Table 1).

During our study the *fss* locus was cloned (see Table 1) and mapped to the same linkage group as $Df^{b380}$ (Nikaido et al., 2002). We performed complementation analysis and found that $Df^{b380}$ and *fss* mutations do not complement, suggesting the $Df^{b380}$ deletion uncovers at least part of the *fss* gene or its regulatory sequences and that at least part of the somite

phenotype of $Df^{b380}$ is due to loss of *fss* function. However, as we describe below, presomitic mesoderm expression of at least one gene differs between $Df^{b380}$ and *fss* mutants, suggesting that the somite defect in $Df^{b380}$ mutants is more severe than in *fss* mutants.

We analysed PMN subtype specification in these different mutants and found that in $Df^{b567}$, $Df^{b380}$ and *fss;yot* mutants *islet2*-expressing and *islet1*-expressing PMNs still form in normal numbers. In addition, both CaP and MiP axons are present, although they often have some aberrant branches, and as in *yot* single mutants, *fss;yot* mutants have fewer PMN axons than wild types (Fig. 2) (van Eeden et al., 1996). However, the precise spacing and alternation of MiPs and CaPs is disturbed in all of these mutants, although the severity of this phenotype varies among embryos and even sometimes between the two sides of the same embryo. In most cases the alternation of MiPs and CaPs is less regular than in wild types, the spacing between PMNs varies and PMNs on the two sides of an embryo are out of register (Fig. 2).

In contrast to the mutants described above, *aei* mutants have a slight 'neurogenic' phenotype in which excess PMNs are produced, resulting in small clusters of *islet2*-expressing and *islet1*-expressing PMNs instead of individual cells (see also Holley et al., 2000). Nevertheless, at 18-20 hpf there is a regular alternation and spacing of *islet1*-expressing and *islet2*-expressing PMNs in *aei* mutants with *islet2*-expressing PMNs forming adjacent to somite middles and *islet1*-expressing PMNs forming adjacent to somite boundaries. This is consistent with observations in other Delta/Notch pathway mutants and embryos expressing a dominant negative Delta construct (Appel and Eisen, 1998; Appel et al., 2001; Gray et al., 2001). The somite defect in *aei* mutants is specific to posterior somites, so we also examined tails of 24 hpf *aei* mutants. Even at this stage, the alternation and spacing of PMNs resembles wild types of a similar stage (compare Fig. 2D with 2E). We also see both CaP and MiP axons in *aei* mutants, although there is aberrant branching posterior to somite 8 (Fig. 2K,L) (van Eeden et al., 1996).

One interpretation of these results is that segmentation of somitic mesoderm is required for fine-tuning or maintaining the spacing and precise alternation of MiPs and CaPs, but is unnecessary for specifying PMN subtypes. However, it is also possible that all of these mutants have some remaining cryptic or early segmentation that is sufficient to specify MiPs and CaPs. Consistent with the latter possibility *cs131*, which encodes a cell cycle arrest protein, is segmentally expressed in presomitic mesoderm of both *aei* and *fss* mutants (Durbin et al., 2000), and *her1* is segmentally expressed in presomitic mesoderm of *fss* mutants, although it is not segmentally expressed in *aei* mutants (Durbin et al., 2000; Holley et al., 2000; van Eeden et al., 1998). We therefore examined expression of *cs131* in $Df^{b567}$, $Df^{b380}$ and *fss;yot* mutants, and expression of *her1* in $Df^{b380}$ and

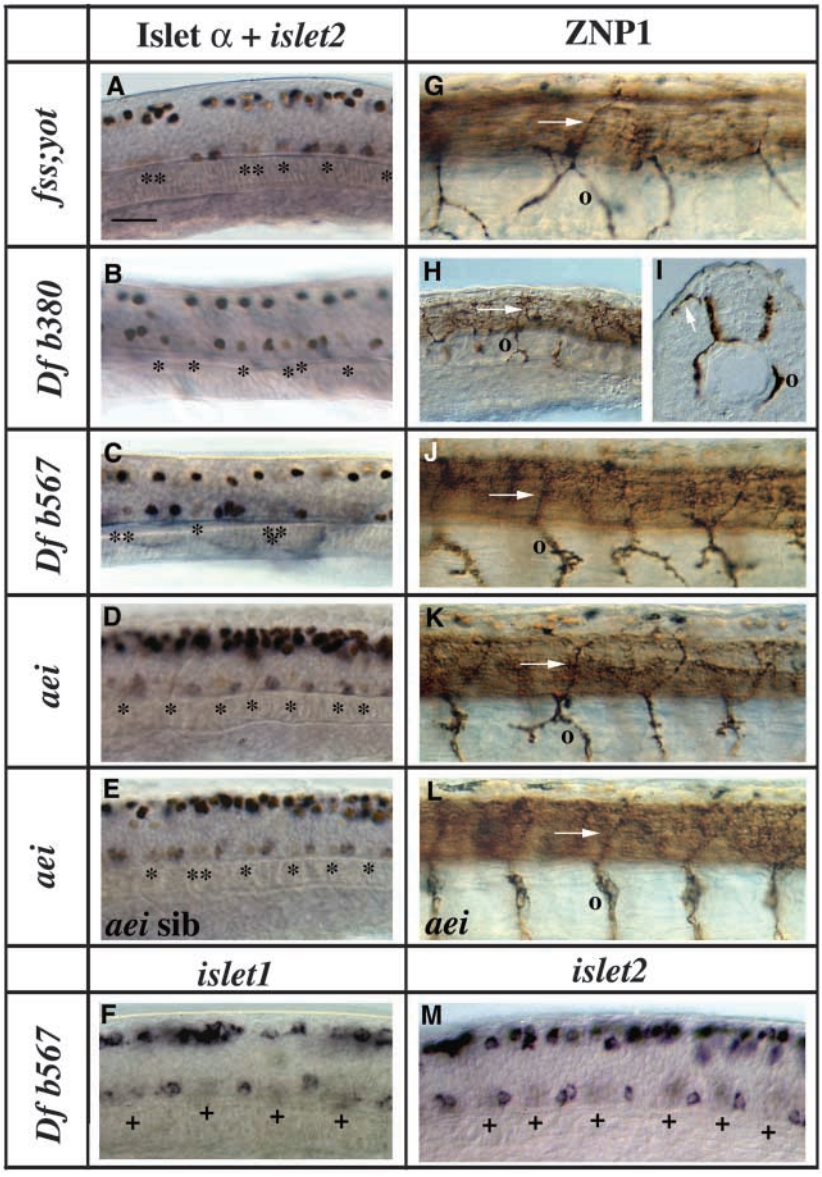


**Fig. 2.** Somite segmentation is unnecessary for MiP and CaP specification. (A-E) Islet antibody + *islet2* in situ hybridization at 18-21 hpf (A-C) and 24 hpf (D,E). Lateral views of the trunk of a *fss;yot* (A), $Df^{b380}$ (B) and $Df^{b567}$ (C) mutant and the tail of an *aei* mutant (D) and an *aei* wild-type sibling (E). Wild-type staining is shown in Fig. 1L. Islet antibody staining is nuclear and brown; *islet2* staining is blue and cytoplasmic; *brown-only cells (MiPs). Comparison of double staining and single in situ hybridization (only shown for $Df^{b567}$; F,M) shows that MiPs and CaPs are specified normally in all of these mutants. (F,M) Lateral views of $Df^{b567}$ mutants. (F) *islet1* in situ hybridization at 16-18 hpf. (M) *islet2* in situ hybridization at 17-19 hpf. In both F and M, out of register PMNs on the other side of the embryo are clearly visible (+), although out of focus. This is never seen in wild types (see Fig. 1B,G). (G-L) znp1 antibody staining at 26-30 hpf. Lateral views of whole-mount *fss;yot* (G), $Df^{b380}$ (H), $Df^{b567}$ (J), and *aei* (K,L) mutants, and cross-section through the trunk of a $Df^{b380}$ mutant (I). Wild-type staining is shown in Fig. 1Q,W. (K) The posterior and (L) anterior of an *aei* mutant trunk. Ventral CaP axons (black circle) and dorsal MiP axons (white arrow) are visible in all cases. Scale bar: 50 μm in A-G,I-M; 25 μm in H.

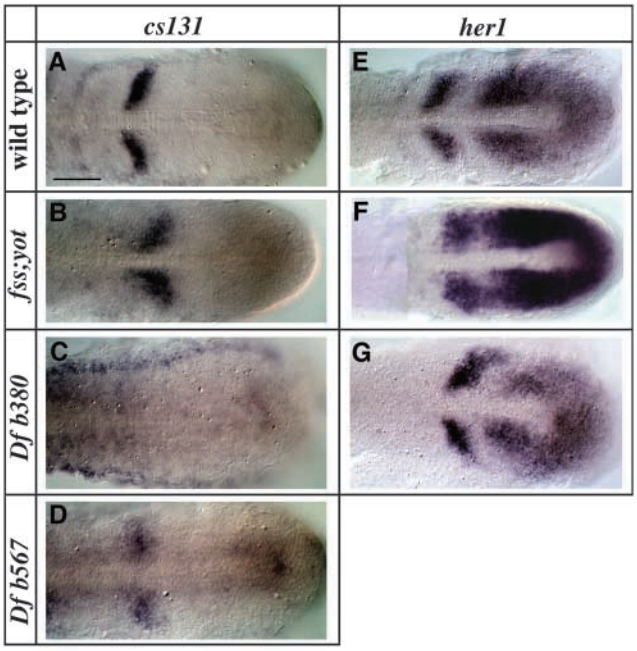


**Fig. 3.** Somite segmentation mutants still have early molecular segmentation. (A-D) *cs131* in situ hybridization at 10-15 somites; (E-G) *her1* in situ hybridization at 8-15 somites. Wild-type embryos (A,E) and *fss;yot* mutants (B,F) all have presomitic mesoderm stripes of both *cs131* and *her1*; $Df^{b380}$ mutants have presomitic mesoderm stripes of *her1* (G) but not *cs131* (C); and $Df^{b567}$ mutants have a presomitic mesoderm stripe of *cs131* (the *her1* gene is deleted in these mutants). In wild-type embryos, there are also weak somitic stripes of *cs131*, but these do not form in *fss;yot*, $Df^{b380}$ or $Df^{b567}$ mutants. Scale bar: 40 μm.

*fss;yot* mutants. In all of these mutants at least one gene is segmentally expressed in presomitic mesoderm. $Df^{b380}$ and *fss;yot* mutants have segmental expression of *her1* in presomitic mesoderm (Fig. 3F,G), and $Df^{b567}$ and *fss;yot* mutants have segmental expression of *cs131* in presomitic mesoderm (Fig. 3B,D). However, compared with wild types in which *cs131* is also expressed in the posterior of each somite, *cs131* expression is weak and unlocalized in somitic mesoderm of these mutants (Fig. 3B-D). By contrast, $Df^{b380}$ mutants lack the presomitic mesoderm stripe of *cs131*, although they still have weak, unlocalized expression of *cs131* in somitic mesoderm (Fig. 3C). This difference in *cs131* expression in presomitic mesoderm of $Df^{b380}$ and *fss;yot* mutants suggests that the somite phenotype of $Df^{b380}$ mutants is more severe than that of *fss* or *fss;yot* mutants. However, even in $Df^{b380}$ mutants, there is still some early molecular segmentation of paraxial mesoderm as evidenced by segmental expression of *her1*.

These results suggest that in addition to signals that specify MiP and CaP subtype identities, there are also signals that fine-tune or maintain correct spatial organization of PMN subtypes and that these signals are missing from somite segmentation mutants. Surprisingly, even though these mutants lack proper segmentation of the somitic mesoderm, CaPs and MiPs are still specified, suggesting that neither somite boundaries, nor AP-restricted gene expression within individual somites are required for PMN subtype specification. However, at least some segmental gene expression remains in presomitic mesoderm in all somite segmentation mutants we examined. This early paraxial mesoderm segmentation may be sufficient to specify MiPs and CaPs, but insufficient for correct spatial organization of these PMN subtypes. Therefore, as no mutations have been described that lack all aspects of paraxial mesoderm segmentation, we examined PMN subtype specification in mutants that lack all paraxial mesoderm.

### Mutants that lack paraxial mesoderm form PMNs with hybrid identities

If signals from either presomitic or somitic mesoderm normally specify PMN subtypes, PMNs should be misspecified in mutants lacking these signals. *spadetail* (*spt*) mutants have a severe reduction of trunk paraxial mesoderm (both somitic and presomitic) and *no tail;spadetail* (*ntl;spt*) mutants completely lack paraxial mesoderm (Amacher et al., 2002; Ho and Kane, 1990) (Table 1). Thus, any signals from presomitic or somitic mesoderm should be reduced in *spt* mutants and completely lacking in *ntl;spt* mutants.

In *ntl;spt* mutants, the vast majority of PMNs express both *islet1* and *islet2* and thus have a hybrid identity with respect to gene expression (Fig. 4A-D; Table 2). An occasional cell expresses just *islet1* (Table 2). These cells may be SMNs that are just initiating *islet1* RNA expression or interneurons that were mistakenly counted as motoneurons because of the misshapen axis in these embryos. By contrast, no PMNs express only *islet2* (0% of PMNs, $n$=251; Fig. 4D). *spt* mutants have a similar but less severe phenotype (Fig. 4E-H; Table 2). Most PMNs express both *islet1* and *islet2* but there are more *islet1*-only expressing cells than in *ntl;spt* mutants (Table 2). In addition, very occasionally in *spt* mutants (1.4% of PMNs, $n$=142) a PMN expresses only *islet2*. We could not analyse the axon trajectories of PMNs in *ntl;spt* mutants, because in the absence of somitic tissue PMN axons do not exit the spinal cord (see also Eisen and Pike, 1991).

In addition to their lack of paraxial mesoderm, *ntl;spt* mutants also lack both notochord and floorplate. Therefore, to check whether these midline structures are required for correct specification of MiPs and CaPs we examined PMN subtype specification in *cyclops;floating head* (*cyc;flh*) mutants that lack both notochord and floorplate (Halpern et al., 1997), and *ntl* single mutants that lack notochord (Halpern et al., 1993); all of these mutants have somitic and presomitic mesoderm. We previously showed that *cyc;flh* mutants have fewer *islet1*-expressing and *islet2*-expressing PMNs due to reduced levels of Hedgehog signalling (Lewis and Eisen, 2001) but we did not assess whether these PMNs have a hybrid identity. In our current study, we found that with respect to both gene expression and axon trajectory, specification of MiPs and CaPs is normal in *cyc;flh* and *ntl* mutants although the spatial organization of these PMNs is sometimes slightly perturbed (Fig. 5).

All of these results are consistent with the hypothesis that signals from paraxial mesoderm specify MiP and CaP subtype identities. They also suggest that in the absence of these signals, PMNs assume a hybrid identity, at least with respect to *islet* gene expression.

### Somites are required for PMN subtype specification

All of the mutants we examined that have a severe somite

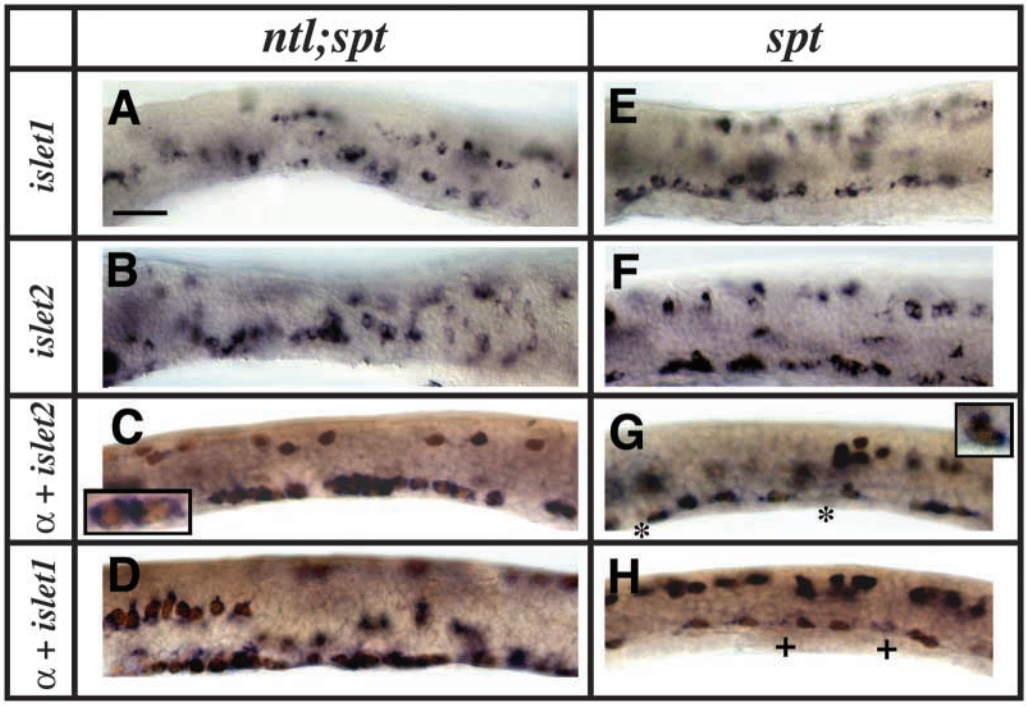


**Fig. 4.** Mutants that lack paraxial mesoderm form hybrid PMNs. (A-D) Lateral views of *ntl;spt* mutant trunks. (E-H) Lateral views of *spt* mutant trunks. (A,E) *islet1* in situ hybridization at 17-18 hpf. In both *spt* and *ntl;spt* mutants, *islet1*-expressing PMNs form continuous rows or clumps. Most of these PMNs also express *islet 2* (see B,C,F,G). (B,F) *islet2* in situ hybridization at 18-20 hpf. In both *spt* and *ntl;spt* mutants, *islet2*-expressing PMNs form continuous rows or clumps.(C,G) Islet antibody + *islet2* in situ hybridization at 18-21 hpf. Islet antibody staining is nuclear and brown; *islet2* staining is blue and cytoplasmic. *Brown-only cell (MiP). Most PMNs in *spt* mutants express *islet2* (only a couple of brown-only cells in G) and almost all PMNs in *ntl;spt* mutants express *islet2* (no brown-only cells in C). Insets show higher magnification of cells with brown and blue staining. (D,H) Islet antibody + *islet1* in situ hybridization at 18-21 hpf. All PMNs in *spt* and *ntl;spt* mutants express *islet1* (there are no brown-only cells in D or H). A small number of cells only express *islet1* RNA (blue-only cells; +); these may be RoPs or SMNs that have just started to express *islet1* RNA but not Islet protein. Scale bar: 50 μm.

phenotype provide strong support for our hypothesis that signals from paraxial mesoderm pattern PMN subtype identities. However, it is still formally possible that mutations in these genes could affect PMNs and somites independently. We tested this possibility by using transplantation methods to create genetically mosaic embryos to ask whether normal PMN subtype identity requires *ntl* and *spt* function in the CNS or in somites. First, we addressed whether wild-type CNS restored normal subtype identities to *ntl;spt* mutant PMNs. We transplanted large numbers of fluorescently labeled, wild-type donor cells into *ntl;spt* MO-injected host embryos at blastula stage (Fig. 6A) and analysed PMN gene expression in eight embryos that lacked somites but in which most trunk spinal cord was derived from wild-type donor cells. In every case, all of the PMNs expressed *islet2*; thus they remained misspecified (Fig. 6B-D). We further analysed four of these embryos in cross-section and confirmed that all PMNs that developed from wild-type donor cells ($n$>40) expressed *islet2* (Fig. 6C,D). These results suggest that wild-type spinal cord cells are insufficient for correct PMN subtype specification in the absence of paraxial mesoderm, consistent with our hypothesis that MiP and CaP subtypes are specified by signals extrinsic to the spinal cord.

Next we addressed whether wild-type somites could restore normal PMN subtype specification in *ntl;spt* mutants. We transplanted fluorescently labeled whole somites from wild-

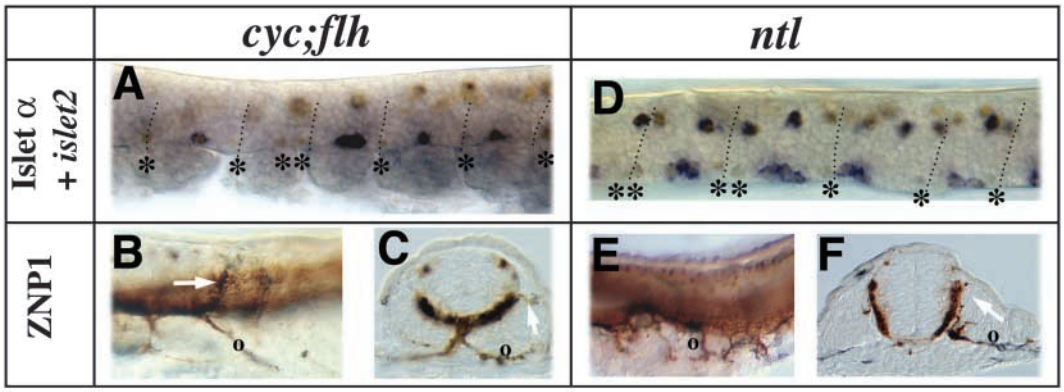


**Fig. 5.** Mutants that lack axial mesoderm specify PMNs normally. (A,B) Lateral views of *cyc;flh* mutant trunks. (C) Cross-section through the anterior trunk of *cyc;flh* mutant. (D) Lateral view of *ntl* single mutant trunk. (E) Lateral view and (F) cross-section of the anterior trunk of a *ntl* single mutant sibling from a *ntl;spt* cross. (A,D) Islet antibody + *islet2* in situ hybridization at 18-21 hpf. Islet antibody staining is nuclear and brown; *islet2* staining is blue and cytoplasmic. *Brown-only cell (MiP). Broken lines indicate somite boundaries. MiPs and CaPs are specified relatively normally in *cyc;flh* (A) and *ntl* (D) mutants. (B,C,E,F) znp1 antibody at 26-30 hpf. Ventral CaP axons are visible in all cases (black circle). MiP axons are visible in some whole mounts and in cross-sections (white arrow). Scale bar: 50 μm.

type donor embryos at the 7-10 somite stage into similarly staged *ntl;spt* mutant or *ntl;spt* MO-injected hosts (Fig. 6E). We carried out this experiment on three separate occasions and each time we restored PMN subtype specification in the region of the somite transplant in at least one embryo. We divided our results into two categories: restoration over two segments (two groups of *islet1*-expressing cells separated by *islet2*-expressing cells) and restoration over more than two segments (restoration of more than two groups of *islet1*-expressing cells separated by *islet2*-expressing cells; Fig. 6F; Table 3). Some transplanted embryos had no restoration of PMN subtype specification. There are a number of technical reasons why this may have been the case: we may have damaged the somites during transplantation, inserted the somites too far from the neural tube, or these host embryos may have been older and PMN fates less labile (Eisen, 1991; Appel et al., 1995). We also processed 28 control embryos: two with transplants in the head, two in which the transplanted somites fell off and 24 *ntl;spt* mutant or MO-injected embryos without transplants processed in parallel to the transplanted embryos.

In a significant number of our transplants, but not in our controls, we restored an alternating pattern of *islet1*-expressing and *islet2*-expressing PMNs in the spinal cord region adjacent to the transplanted wild-type somites (Fig. 6F; Table 3). In cases in which we could see somite boundaries, *islet1*-expressing PMNs were located adjacent to these boundaries, whereas *islet2*-expressing PMNs were located between them (Fig. 6E). These results show that lack of paraxial mesoderm in *ntl;spt* mutants causes mis-specification of PMN subtypes, therefore specification of MiPs and CaPs requires signals from paraxial mesoderm.

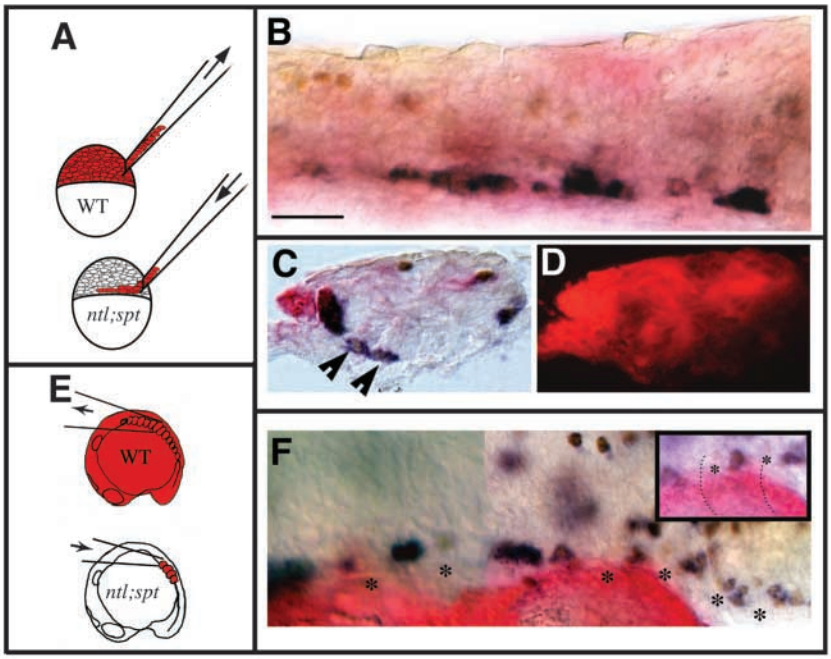


**Fig. 6.** Somite transplants restore the normal PMN subtype pattern in *ntl;spt* mutants. (A) Schematic of blastula stage transplants. (B-D,F) Islet antibody + *islet2* in situ hybridization + anti-fluorescein antibody staining at 18-22 hpf. Islet antibody staining is nuclear and brown; *islet2* staining is blue and cytoplasmic; red staining is fluorescent and shows wild-type donor cells that contain fluorescein dextran. Brown-only cells (*) express only *islet1* and hence are MiPs; blue + brown cells express *islet2* and possibly also *islet1*, and are therefore CaPs or hybrid PMNs. (B) *ntl;spt* MO-injected host embryo with its spinal cord completely filled with wild-type donor cells but devoid of wild-type somite cells. No MiPs (brown-only cells) are present in this embryo, so the PMNs probably still all have a hybrid identity. (C) Bright-field microscopy and (D) fluorescence microscopy of the same cross-section of another *ntl;spt* MO-injected host embryo with its spinal cord completely filled with wild-type donor cells but devoid of wild-type somite cells. Two triple-labeled PMNs are indicated with arrowheads. (E) Schematic of whole somite transplants. (F) *ntl;spt* MO-injected host embryo with transplanted wild-type somites. Several MiPs (brown-only cells; *) are present adjacent to the wild-type somites (red). These MiPs are separated by blue + brown cells that are probably CaPs. Insert shows a different *ntl;spt* host embryo with transplanted wild-type somites; in this case, the somite boundaries are clearly visible (broken lines). As in wild-type embryos, MiPs were adjacent to these somite boundaries. Scale bar: 50 μm.

## Discussion

We provide the first analysis of how a segmentally reiterated pattern of neurons is specified along the AP axis of the vertebrate spinal cord by analysing how CaP and MiP motoneuron subtypes are specified and spatially organized in embryonic zebrafish. These different PMN subtypes occupy different locations within the ventral spinal cord relative to overlying somites, express different genes and innervate different muscle territories (Lewis and Eisen, 2003). We show that signals from paraxial mesoderm specify this reiterated, segmental pattern of zebrafish PMN subtypes. In the absence of these signals, PMNs express both *islet1* and *islet2*, and hence have a hybrid identity with respect to gene expression; under these conditions, the CaP axon trajectory appears dominant. Our results also suggest that there is a distinct mechanism for

**Table 3. Wild-type somites restore PMN subtype specification in *ntl;spt* mutants**

| Experimental condition | Total number of embryos | Restored PMN subtype specification in more than two segments | Restored PMN subtype specification in two segments | No restoration of PMN subtype specification |
|---|---|---|---|---|
| Transplanted embryos | 14 | 4 | 5 | 5 |
| Control embryos | 28 | 0 | 2 | 26 |

A Likelihood Ratio Test showed that PMN subtype specification was significantly different in transplanted embryos when compared with controls (4/14 versus 0/28 and 9/14 versus 2/28; $P<0.002$).

ensuring correct spatial organization of PMN subtypes that requires at least some aspects of normal somite segmentation.

### Signals from paraxial mesoderm specify MiPs and CaPs

Our evidence that signals from paraxial mesoderm are required for correct specification of MiPs and CaPs is threefold. First, our analysis of *tri;kny* mutants shows a correlation between very narrow somites and misspecified PMNs. Second, our analysis of *ntl;spt* and *spt* mutants shows a correlation between loss of paraxial mesoderm (presomitic mesoderm and somites) and mis-specification of PMNs. Third, our transplantation experiments demonstrate that mis-specification of PMN subtypes in *ntl;spt* mutants is caused by lack of paraxial mesoderm.

Our analysis of PMNs in *spt* mutants is consistent with previously published data. Inoue et al. (Inoue et al., 1994) reported an increase in *islet1*-expressing MNs in *spt* mutants at 24 hpf and Bisgrove et al. (Bisgrove et al., 1997) reported an increase in *islet2*-expressing PMNs at 18 hpf. Both of these observations are consistent with our findings that most PMNs in *spt* mutants express both *islet1* and *islet2* at 18-20 hpf. However, Tokumoto et al. (Tokumoto et al., 1995) reported a reduction in the number of *islet2*-expressing MNs in *spt* mutants slightly later, at 24 hpf. This is surprising, given our results and those of Bisgrove et al. (Bisgrove et al., 1997). However, it is possible that SMNs, some of which also express *islet2* by 24 hpf, are reduced or delayed, or that some PMNs are dying, resulting in a reduction in *islet2*-expressing MNs at this later stage.

### Why are *tri;kny* and *ntl;spt* mutant phenotypes so similar?

*tri;kny* mutants form PMNs with a hybrid identity as assayed by *islet* gene expression. The simplest interpretation of this result is that there are two signals from the paraxial mesoderm, one that induces or maintains *islet1* expression in MiPs and one that induces *islet2* expression in CaPs. In wild-type embryos, these signals are spatially distinct so that each PMN experiences only one of them. By contrast, in *tri;kny* mutants these signals are so close together that they overlap and all PMNs experience both signals and respond by expressing both *islet* genes. The idea of inducing signals is supported by experiments showing that individual MiPs transplanted to the CaP position turn on expression of *islet2*. These experiments suggest that localized signals normally induce *islet2* expression in CaPs (Appel et al., 1995; Eisen, 1991), and also demonstrate that PMNs that do not normally experience this *islet2*-inducing signal still have the ability to respond to it.

In the light of these results, it was surprising to find that in *ntl;spt* mutants that lack all paraxial mesoderm-derived signals, PMNs also express both *islet1* and *islet2*. The simplest interpretation of this result is that there are two signals from paraxial mesoderm: one that normally represses *islet2* expression in MiPs and one that normally represses *islet1* expression in CaPs. This simple model, with two repressive signals, is inconsistent with the simple model suggested by the *tri;kny* double mutant and PMN transplantation results, which postulated two inducing signals. This suggests to us that the signalling that specifies CaP and MiP subtypes may involve both repressive and inductive signals, and hence be more complicated than either of these simple models. Thus, although our results demonstrate that signals from paraxial mesoderm are required for PMN subtype specification, it is still unclear exactly how these signals act. Further studies will be needed to identify these signals and the mechanisms by which they specify distinct PMN subtypes.

### CaP axon trajectory may be dominant in PMNs that express both *islet1* and *islet2*

In *tri;kny* mutants most PMNs express both *islet1* and *islet2* but have a CaP axon trajectory, suggesting that CaP identity is dominant over MiP identity. *tri;kny* mutants do have rare PMNs with a MiP-like axon trajectory that probably correspond to the occasional PMNs that express only *islet1*. However, an intriguing possibility that remains to be tested is that, as suggested from studies in mouse, over-occupation of a particular axon pathway may cause an occasional axon to be 'shunted' to an alternative target (Sharma et al., 2000).

We offer three possible interpretations of why PMNs in *tri;kny* mutants have CaP-like axons despite their hybrid subtype identity as indicated by gene expression. First, somite-derived signals necessary for MiP axon pathfinding may be lacking in *tri;kny* mutants. This seems unlikely as the occasional MiP-like axon still forms, and all of the genes examined so far are expressed normally in the somites of these mutants (Henry et al., 2000) (K.E.L. and J.S.E., unpublished). Second, CaP-specifying signals may be dominant over MiP-specifying signals and even though PMNs in *tri;kny* mutants express both *islet1* and *islet2*, they may otherwise molecularly resemble CaPs more than MiPs. This possibility can be assessed when additional molecular markers for PMN subtypes are identified. A third related possibility is that expression of *islet2* may specify a CaP-like axon trajectory in PMNs, irrespective of other *islet* genes the cell expresses. We favor this possibility, because it is consistent with studies showing that reducing Islet2 function changes CaPs into VeLD spinal interneurons (Segawa et al., 2001).

### Somite segmentation is required for correct spatial organization of MiPs and CaPs

To our initial surprise, both MiPs and CaPs were specified in normal numbers in mutants with disturbed somite boundaries and AP somite patterning. This suggests that neither of these aspects of paraxial mesoderm segmentation are required to specify different PMN subtypes, although we cannot rule out the possibility that there are as yet unidentified genes expressed segmentally in the somites of these mutants. Interestingly, although MiPs and CaPs formed in all of these mutants, in most cases their spatial organization was disturbed. The precise alternation and spacing of different PMN subtypes was lost and PMNs on the two sides of an embryo were out of register. This shows that PMN subtype specification and PMN spatial organization are separable aspects of PMN patterning and it suggests that these somite segmentation mutants are missing signals that normally fine-tune or maintain the precise spatial organization of different PMN subtypes. One mechanism by which these signals may act is by controlling the cell adhesion properties of particular PMNs and/or neighboring cells. In this model the normal, precise, alternating pattern of MiPs and CaPs would be fine-tuned or maintained by cell adhesion and this mechanism would be disturbed or lacking in the somite segmentation mutants. This would explain why transplanted PMNs sometimes migrate back to their original spinal cord

positions relative to overlying somites (Eisen, 1991). In addition, if these cell adhesion properties develop after CaPs are first specified, it would explain why the initial spatial organization of CaPs is not as regular as at later stages (Appel et al., 1995).

### What are the signals for PMN subtype specification and when do they act?

When we started our analyses, one large class of genes that were obvious candidates for specifying PMN subtype identities were genes that are normally expressed in an AP-restricted pattern in somites. However, all of these genes that have been examined so far are either not expressed, or are mislocalized in somite segmentation mutants (Durbin et al., 2000; Henry et al., 2002; Holley et al., 2000; Jiang et al., 2000; van Eeden et al., 1996). Yet both MiPs and CaPs form in normal numbers in these mutants. This strongly suggests that none of these genes are required for specifying PMN subtypes.

The signals that normally specify MiPs and CaPs might emanate from presomitic mesoderm. Consistent with this possibility, although the somite segmentation mutants we examined affect different aspects of paraxial mesoderm segmentation, in every case at least one gene is still segmentally expressed in presomitic mesoderm. If the signals that specify PMN subtypes come from presomitic mesoderm, MiPs and CaPs would be specified before we can currently identify them molecularly. However, if PMN subtypes are specified this early, additional, somite-derived signals would be required to explain how PMNs transplanted at mid-somitogenesis stages can adopt a new, position-specific PMN subtype identity (Appel et al., 1995; Eisen, 1991) and transplanted somites can restore specification of PMN subtype identities in *ntl;spt* mutants. These later signals might normally only fine-tune the spatial organization of MiPs and CaPs, in which case they are presumably missing in the somite segmentation mutants.

An alternative possibility is that signals that specify MiPs and CaPs emanate from the somites. In this case, there must be some cryptic aspect of segmentation that persists in the somitic mesoderm in somite segmentation mutants that is sufficient to specify MiPs and CaPs. Consistent with this possibility, vertebrae form with almost normal periodicity in these mutants, and most of the mutants form irregular myotome boundaries at later developmental stages (van Eeden et al., 1996; van Eeden et al., 1998). Distinguishing between these two alternatives will require the identification of additional genes involved in segmentation and in PMN subtype specification.

FGFs are another class of signals that might be candidates for specifying PMN subtype identities. FGF signalling is crucial for somite segmentation (Dubrulle and Pourquie, 2002) and correct timing of neural differentiation (Diez del Corral et al., 2002), and has also been implicated in AP patterning of MNs in chick (Liu et al., 2001). In zebrafish, *fgf8* is expressed in the posterior presomitic mesoderm and in the anterior region of newly formed somites (Reifers et al., 1998). *fgf17* is also expressed at the anterior margin of somites after about the eight-somite stage (Reifers et al., 2000). However, our preliminary data show that, although somite boundaries are variably disturbed in embryos with reduced FGF8 signalling, MiPs and CaPs are specified normally in *ace* (*fgf8*) mutants, embryos injected with *fgf8* MOs and *ace* mutants injected with an *fgf17* MO. However, in some of these embryos, PMN spacing is irregular and PMNs on the two sides of an embryo are out of register in a manner reminiscent of somite segmentation mutants (K.E.L. and J.S.E., unpublished). Our treatments have probably not entirely abolished FGF signalling. Thus, we have not ruled out the possibility that FGFs participate in PMN subtype specification, although this may be difficult to assess because embryos become highly necrotic when *fgf8* levels are severely reduced (Draper et al., 2001) (K.E.L. and J.S.E., unpublished).

In conclusion, our data provide strong evidence that signals from paraxial mesoderm are required to specify and spatially organise distinct PMN subtypes in a segmentally reiterated pattern along the AP axis. It will be exciting in the future to learn the nature of the signals involved in these processes and when and how they act during PMN subtype specification.

We thank Michael Brand, Sharon Amacher, Bruce Draper and Jon Muyskens for sharing MOs prior to publication; Roger Albertson for help with some initial analysis of $Df^{b567}$; Sharon Amacher for sharing this line with us prior to publication; Christoph Winkler for sharing the *nkx2.2b* probe prior to publication; the staff of the UO Histology Facility for help with sectioning; and Alan Arnett, Martha Jones, Ellie Melançon, Chapell Miller, Mary Swartz and the staff of the UO Zebrafish Facility for fish husbandry. We also thank Bruce Appel, Estelle Hirsinger, Julie Kuhlman, Lisa Maves and Monte Westerfield for comments on previous versions of this manuscript. Supported by NIH grants NS23915 and HD22486 and Wellcome International Prize Travelling Research Fellowship 054975 to K.E.L.

## References

**Amacher, S. L., Draper, B. W., Summers, B. R. and Kimmel, C. B.** (2002). The zebrafish T-box genes *no tail* and *spadetail* are required for development of trunk and tail mesoderm and medial floor plate. *Development* **129**, 3311-3323.

**Appel, B. and Eisen, J.** (1998). Regulation of neuronal specification in the zebrafish spinal cord by *Delta* function. *Development* **125**, 371-380.

**Appel, B., Korzh, V., Glasgow, E., Thor, S., Edlund, T., Dawid, I. B. and Eisen, J. S.** (1995). Motoneuron fate specification revealed by patterned LIM homeobox gene expression in embryonic zebrafish. *Development* **121**, 4117-4125.

**Appel, B., Givan, L. A. and Eisen, J. S.** (2001). Delta-Notch signaling and lateral inhibition in zebrafish spinal cord development. *BMC Dev. Biol.* **1**, 13.

**Beattie, C. and Eisen, J.** (1997). Notochord alters the permissiveness of myotome for pathfinding by an identified motoneuron in embryonic zebrafish. *Development* **124**, 713-720.

**Bisgrove, B., Raible, D., Walter, V., Eisen, J. and Grunwald, D.** (1997). Expression of c-ret in the zebrafish embryo: potential roles in motoneuronal development. *J. Neurobiol.* **33**, 749-768.

**Concordet, J. P., Lewis, K. E., Moore, J. W., Goodrich, L. V., Johnson, R. L., Scott, M. P. and Ingham, P. W.** (1996). Spatial regulation of a zebrafish patched homologue reflects the roles of sonic hedgehog and protein kinase A in neural tube and somite patterning. *Development* **122**, 2835-2846.

**Diez del Corral, R., Breitkreuz, D. N. and Storey, K. G.** (2002). Onset of neuronal differentiation is regulated by paraxial mesoderm and requires attenuation of FGF signalling. *Development* **129**, 1681-1691.

**Draper, B. W., Morcos, P. A. and Kimmel, C. B.** (2001). Inhibition of zebrafish fgf8 pre-mRNA splicing with morpholino oligos: A quantifiable method for gene knockdown. *Genesis* **30**, 154-156.

**Dubrulle, J. and Pourquie, O.** (2002). From head to tail: links between the segmentation clock and antero-posterior patterning of the embryo. *Curr. Opin. Genet. Dev.* **12**, 519-523.

**Durbin, L., Sordino, P., Barrios, A., Gering, M., Thisse, C., Thisse, B., Brennan, C., Green, A., Wilson, S. and Holder, N.** (2000). Anterior-posterior patterning of somites is required within segments for somite boundary formation in developing zebrafish. *Development* **127**, 1703-1713.

**Eisen, J. S.** (1991). Determination of primary motoneuron identity in developing zebrafish embryos. *Science* **252**, 569-572.

**Eisen, J. S.** (1994). Development of motoneuronal phenotype. *Ann. Rev. Neurosci.* **17**, 1-30.

**Eisen, J. S.** (1999). Patterning motoneurons in the vertebrate nervous system. *Trends Neurosci.* **22**, 321-326.

**Eisen, J. S. and Pike, S. H.** (1991). The *spt-1* mutation alters the segmental arrangement and axonal development of identified neurons in the spinal cord of the embryonic zebrafish. *Neuron* **6**, 767-776.

**Eisen, J. S., Pike, S. H. and Debu, B.** (1989). The growth cones of identified motoneurons in embryonic zebrafish select appropriate pathways in the absence of specific cellular interactions. *Neuron* **2**, 1097-1104.

**Ensini, M., Tsuchida, T. N., Belting, H.-G. and Jessell, T. M.** (1998). The control of rostrocaudal pattern in the developing spinal cord: specification of motor neuron subtype identity is initiated by signals from paraxial mesoderm. *Development* **125**, 969-982.

**Fritz, A., Rozowski, M., Walker, C. and Westerfield, M.** (1996). Identification of selected gamma-ray induced deficiencies in zebrafish using multiplex polymerase chain reaction. *Genetics* **144**, 1735-1745.

**Gray, M., Moens, C. B., Amacher, S. L., Eisen, J. S. and Beattie, C. E.** (2001). Zebrafish deadly seven functions in neurogenesis. *Dev. Biol.* **237**, 306-323.

**Griffin, K. J. P., Amacher, S. L., Kimmel, C. B. and Kimelman, D.** (1998). Molecular identification of *spadetail*: regulation of zebrafish trunk and tail mesoderm formation by *T-box* genes. *Development* **125**, 3379-3388.

**Halpern, M. E., Ho, R. K., Walker, C. and Kimmel, C. B.** (1993). Induction of muscle pioneers and floor plate is distinguished by the zebrafish *no tail* mutation. *Cell* **75**, 99-111.

**Halpern, M., Hatta, K., Amacher, S., Talbot, W., Yan, Y., Thisse, B., Thisse, C., Postlethwait, J. and Kimmel, C.** (1997). Genetic interactions in zebrafish midline development. *Dev. Biol.* **187**, 154-170.

**Hammerschmidt, M., Pelegri, F., Mullins, M. C., Kane, D. A., Brand, M., van Eeden, F. J. M., Furutani-Seiki, M., Granato, M., Haffter, P., Heisenberg, C. P. et al.** (1996). Mutations affecting morphogenesis during gastrulation and tail formation in the zebrafish, *Danio rerio*. *Development* **123**, 143-151.

**Hatta, K., Kimmel, C. B., Ho, R. K. and Walker, C.** (1991). The *cyclops* mutation blocks specification of the floor plate of the zebrafish CNS. *Nature* **350**, 339-341.

**Henry, C. A., Hall, L. A., Hille, M. B., Solinca-Krezel, L. and Cooper, M. S.** (2000). Somites in zebrafish doubly mutant for *knypek* and *trilobite* form without internal mesenchymal cells or compaction. *Curr. Biol.* **10**, 1063-1066.

**Henry, C. A., Urban, M. K., Dill, K. K., Merlie, J. P., Page, M. F., Kimmel, C. B. and Amacher, S. L.** (2002). Two linked hairy/Enhancer of split-related zebrafish genes, her1 and her7, function together to refine alternating somite boundaries. *Development* **129**, 3693-3704.

**Ho, R. K. and Kane, D. A.** (1990). Cell-autonomous action of zebrafish spt-1 mutation in specific mesodermal precursors. *Nature* **348**, 728-730.

**Holley, S. A., Geisler, R. and Nusslein-Volhard, C.** (2000). Control of her1 expression during zebrafish somitogenesis by a delta-dependent oscillator and an independent wave-front activity. *Genes Dev.* **14**, 1678-1690.

**Inoue, A., Takahashi, M., Hatta, K., Hotta, Y. and Okamoto, H.** (1994). Developmental regulation of *islet-1* mRNA expression during neuronal differentiation in embryonic zebrafish. *Dev. Dyn.* **199**, 1-11.

**Jessen, J. R., Topczewski, J., Bingham, S., Sepich, D. S., Marlow, F., Chandrasekhar, A. and Solnica-Krezel, L.** (2002). Zebrafish trilobite identifies new roles for Strabismus in gastrulation and neuronal movements. *Nat. Cell Biol.* **4**, 610-615.

**Jiang, Y. J., Aerne, B. L., Smithers, L., Haddon, C., Ish-Horowicz, D. and Lewis, J.** (2000). Notch signalling and the synchronization of the somite segmentation clock. *Nature* **408**, 475-479.

**Karlstrom, R. O., Tyurina, O. V., Kawakami, A., Nishioka, N., Talbot, W. S., Sasaki, H. and Schier, A. F.** (2003). Genetic analysis of zebrafish gli1 and gli2 reveals divergent requirements for gli genes in vertebrate development. *Development* **130**, 1549-1564.

**Kimmel, C. B., Ballard, W. W., Kimmel, S. R., Ullmann, B. and Schilling, T. F.** (1995). Stages of embryonic development of the zebrafish. *Dev. Dyn.* **203**, 253-310.

**Kimmel, C. B., Sepich, D. S. and Trevarrow, B.** (1988). Development of segmentation in zebrafish. *Development Suppl.* **104**, 197-207.

**Lewis, K. E., Currie, P. D., Roy, S., Schauerte, H., Haffter, P. and Ingham, P. W.** (1999). Control of muscle cell-type specification in the zebrafish embryo by hedgehog signalling. *Dev. Biol.* **216**, 469-480.

**Lewis, K. E. and Eisen, J. S.** (2001). Hedgehog signaling is required for primary motoneuron induction in zebrafish. *Development* **128**, 3485-3495.

**Lewis, K. E. and Eisen, J. S.** (2003). From cells to circuits: development of the zebrafish spinal cord. *Prog. Neurobiol.* **69**, 419-449.

**Liu, D., Chu, H., Maves, L., Yan, Y. L., Morcos, P. A., Postlethwait, J. H. and Westerfield, M.** (2003). Fgf3 and Fgf8 dependent and independent transcription factors are required for otic placode specification. *Development* **130**, 2213-2224.

**Liu, J. P., Laufer, E. and Jessell, T. M.** (2001). Assigning the positional identity of spinal motor neurons: rostrocaudal patterning of Hox-c expression by FGFs, Gdf11, and retinoids. *Neuron* **32**, 997-1012.

**Müller, M., Weizsäcker, E. and Campos-Ortega, J. A.** (1996). Expression domains of a zebrafish homologue of the *Drosophila* pair-rule gene *hairy* correspond to a primordia of alternating somites. *Development* **122**, 2071-2078.

**Nasevicius, A. and Ekker, S. C.** (2000). Effective targeted gene 'knockdown' in zebrafish. *Nat. Genet.* **26**, 216-220.

**Nikaido, M., Kawakami, A., Sawada, A., Furutani-Seiki, M., Takeda, H. and Araki, K.** (2002). Tbx24, encoding a T-box protein, is mutated in the zebrafish somite-segmentation mutant fused somites. *Nat. Genet.* **31**, 195-199.

**Odenthal, J., van Eeden, F. J., Haffter, P., Ingham, P. W. and Nüsslein-Volhard, C.** (2000). Two distinct cell populations in the floor plate of the zebrafish are induced by different pathways. *Dev. Biol.* **219**, 350-363.

**Rebagliati, M. R., Toyama, R., Haffter, P. and Dawid, I. B.** (1998). *Cyclops* encodes a nodal-related factor in midline signaling. *Proc. Natl. Acad. Sci. USA* **95**, 9932-9937.

**Reifers, F., Adams, J., Mason, I., Schulte-Merker, S. and Brand, M.** (2000). Overlapping and distinct functions provided by fgf17, a new zebrafish member of the Fgf8/17/18 subgroup of Fgfs. *Mech. Dev.* **99**, 39-49.

**Reifers, F., Böhli, H., Walsh, E. C., Crossley, P. H., Stainier, D. Y. and Brand, M.** (1998). Fgf8 is mutated in zebrafish acerebellar (ace) mutants and is required for maintenance of midbrain-hindbrain boundary development and somitogenesis. *Development* **125**, 2381-2395.

**Roy, M. N., Prince, V. E. and Ho, R. K.** (1999). Heat shock produces periodic somitic disturbances in the zebrafish embryo. *Mech. Dev.* **85**, 27-34.

**Sampath, K., Rubinstein, A. L., Cheng, A. M. S., Liange, J. O., Fekany, K., Solnica-Krezel, L., Korzh, V., Halpern, M. E. and Wright, C. V. E.** (1998). Induction of the zebrafish ventral brain and floor plate requires *Cyclops*/*Nodal* signaling. *Nature* **395**, 185-189.

**Schulte-Merker, S., van Eeden, F., Halpern, M., Kimmel, C. and Nüsslein-Vohlard, C.** (1994). *no tail* (*ntl*) is the zebrafish homologue of the mouse T (*Brachyury*) gene. *Development* **120**, 1009-1015.

**Segawa, H., Miyashita, T., Hirate, Y., Higashijima, S., Chino, N., Uyemura, K., Kikuchi, Y. and Okamoto, H.** (2001). Functional repression of Islet-2 by disruption of complex with Ldb impairs peripheral axonal outgrowth in embryonic zebrafish. *Neuron* **30**, 423-436.

**Sepich, D. S., Myers, D. C., Short, R., Topczewski, J., Marlow, F. and Solnica-Krezel, L.** (2000). Role of the zebrafish trilobite locus in gastrulation movements of convergence and extension. *Genesis* **27**, 159-173.

**Sharma, K., Leonard, A. E., Lettieri, K. and Pfaff, S. L.** (2000). Genetic and epigenetic mechanisms contribute to motor neuron pathfinding. *Nature* **406**, 515-519.

**Talbot, W. S., Trevarrow, B., Halpern, M., Melby, A. E., Farr, G., Postlethwait, J. H., Jowett, T., Kimmel, C. B. and Kimmelman, D.** (1995). A homeobox gene essential for zebrafish notochord development. *Nature* **378**, 150-157.

**Tokumoto, M., Gong, Z., Tsubokawa, T., Hew, C. L., Uyemura, K., Hotta, Y. and Okamoto, H.** (1995). Molecular heterogeneity among primary motoneurons and within myotomes revealed by the differential mRNA expression of novel *islet-1* homologs in embryonic zebrafish. *Dev. Biol.* **171**, 578-589.

**Topczewski, J., Sepich, D. S., Myers, D. C., Walker, C., Amores, A., Lele, Z., Hammerschmidt, M., Postlethwait, J. H. and Solnica-Krezel, L.** (2001). The zebrafish glypican Knypek controls cell polarity during gastrulation movements of convergent extension. *Dev. Cell* **1**, 251-264.

**Trevarrow, B., Marks, D. L. and Kimmel, C. B.** (1990). Organization of hindbrain segments in the zebrafish embryo. *Neuron* **4**, 669-679.

**van Eeden, F. J. M., Granato, M., Schach, U., Brand, M., Furutani-Seiki, M., Haffter, P., Hammerschmidt, M., Heisenberg, C. P., Jiang, Y. J., Kane, D. A. et al.** (1996). Mutations affecting somite formation and patterning in the zebrafish, *Danio rerio*. *Development* **123**, 153-164.

**van Eeden, F. J. M., Holley, S. A., Haffter, P. and Nusslein-Volhard, C.** (1998). Zerafish segmentation and pair-rule patterning. *Dev. Genet.* **23**, 65-76.